1 Facility Status

1-1 Accelerators

Two electron storage rings, the PF-ring and the PF-AR, as dedicated light sources were stably operated at the Photon Factory. The KEK linear accelerator with maximum electron energy of 8 GeV is employed to inject the electron beam into the rings. The full energy injection of 2.5 GeV is carried out at the PF-ring, while it is required to increase the energy from the injection energy of 3 GeV to the operation energy of 6.5 GeV at the PF-AR.

The machine parameters of the rings and the calculated spectral performances are listed in Table 1 and Table 2, respectively. The spectral distributions of synchrotron radiation (SR) from the bending magnets and the insertion devices are shown in Fig. 1

Table 1: Principal beam parameters of the PF ring and PF-AR.

	PF	PF-AR
Energy	2.5 GeV	6.5 GeV
Natural emittance	34.6 nm rad	293 nm rad
Circumference	187 m	377 m
RF frequency	500.1 MHz	508.6 MHz
Bending radius	8.66 m	23.2 m
Energy loss per turn	0.4 MeV	6.66 MeV
Damping time		
Vertical	7.8 ms	2.5 ms
Longitudinal	3.9 ms	1.2 ms
Natural bunch length	10 mm	18.6 mm
Momentum compaction factor	0.00644	0.0129
Natural chromaticity		
Horizontal	12.9	-14.3
Vertical	-17.3	-13.1
Stored current	450 mA	60 mA
Number of bunches	252	1
Beam lifetime	20-25 h (at 450 mA)	20-25 h (at 60 mA)

Table 2: Calculated spectral performances of the bend source and all the insertion devices at the PF ring (2.5 GeV, 450 mA) and the PF-AR (6.5 GeV, 60 mA). λ_u: period length, *N*: number of the periods, *L*: length of undulator or wiggler, $G_y(G_x)$: minimum vertical (horizontal) gap height, $B_y(B_x)$: maximum vertical (horizontal) magnetic field, Type of magnet, H: hybrid configuration, S.C.: super conducting magnet, σ_x,σ_y: horizontal or vertical beam size, σ_x',σ_y': horizontal or vertical beam divergence, $K_y(K_x)$: vertical (horizontal) deflection parameter, *D*: photon flux density (photons/sec/mrad^2/0.1%b.w.), *B*: brilliance (photons/sec/mm^2/mrad^2/0.1%b.w.), P_T:total radiated power. Different operating modes of undulator and wiggler are denoted by -U and -W, respectively

Name	E/I	λ_u	N	L	$G_y(G_x)$	$B_y(B_x)$	Type of magnet	σ_x	σ_y	$\sigma_{x'}$	$\sigma_{y'}$	$K_y(K_x)$	$\varepsilon_1/\varepsilon_c$	D	B	P_T
	GeV/mA	cm		m	cm	T		mm	mm	mrad	mrad		keV			kW
PF	**2.5/450**															
Bend								0.41	0.059	0.178	0.012		4	5.38E+13	3.48E+14	
SGU#01		1.2	39	0.5	0.4	0.7	P(NdFeB)	0.6	0.012	0.088	0.029	0.78		4.56E+16	9.90E+17	0.4
U#02-1		6	60	3.6	2.8	0.4	H(NdFeB)	0.65	0.042	0.054	0.008	2.3		2.73E+17	1.55E+18	1.07
U#02-2		16	17	2.72	2.6	0.33(0.33)	P(NdFeB)	0.65	0.042	0.054	0.008	4.93(4.93)		9.53E+15	4.58E+16	0.53
SGU#03		1.8	26	0.5	0.4	1	P(NdFeB)	0.6	0.012	0.088	0.029	1.68		2.50E+16	5.44E+17	0.82
MPW#05-W		12	21	2.5	2.64	1.4	H(NdFeB)	0.71	0.045	0.078	0.009	16	5.9	2.22E+15	1.10E+16	8.83
U#13		7.6	47	3.6	2.3	0.74(0.51)	P(NdFeB)	0.74	0.02	0.094	0.019	5.28(3.65)		4.46E+16	3.10E+17	3.53
VW#14					5	5	S.C.	0.53	0.045	0.128	0.008		20.8	5.42E+13	3.59E+14	
SGU#15		1.76	27	0.5	0.4	0.97	P(NdFeB)	0.6	0.012	0.088	0.029	1.37		4.38E+15	9.44E+16	0.75
U#16-1 & 16-2		5.6	44	2.5	2.1	0.6(0.38)	P(NdFeB)	0.654	0.042	0.055	0.008	3(2)		1.03E+18	1.82E+17	0.88
SGU#17		1.6	29	0.5	0.4	0.92	P(NdFeB)	0.6	0.012	0.088	0.029	1.37		7.88E+15	1.71E+17	0.69
Revolver#19-B		7.2	32	3.6	2.8	0.4	H(NdFeB)	0.7	0.045	0.078	0.009	2.7		7.17E+16	3.52E+17	0.63
U#28		16	22	3.52	2.7	0.33(0.33)	P(NdFeB)	0.53	0.045	0.127	0.008	4.93(4.93)		1.39E+16	6.59E+16	1.36
PF-AR	**6.5/60**															
Bend								1	0.2	0.593	0.036		26	3.90E+13	3.11E+13	
EMPW#NE01-W		16	21	3.36	3(11)	1(0.2)	P(NdFeB)	1.07	1.07	0.268	0.032	15(3)	28(90%)	1.84E+15	2.54E+15	5.52
U#NE03		4	90	3.6	1	0.8	P(NdFeB)	1.57	0.17	0.312	0.029	3		1.29E+16	7.66E+15	3.708
U#NW02		4	90	3.6	1	0.8	P(NdFeB)	1.57	0.17	0.312	0.029	3		1.29E+16	7.66E+15	3.708
U#NW12		4	95	3.8	1	0.8	P(NdFeB)	1.57	0.17	0.312	0.029	3		1.29E+16	7.66E+15	3.912
U#NW14-36		3.6	79	2.8	1	0.8	P(NdFeB)	1.35	0.14	0.338	0.036	2.8		7.69E+15	6.49E+15	3.12
U#NW14-20		2	75	1.5	0.8	0.63	P(NdFeB)	0.75	0.07	0.383	0.038	1.17		7.69E+15	6.49E+15	0.936

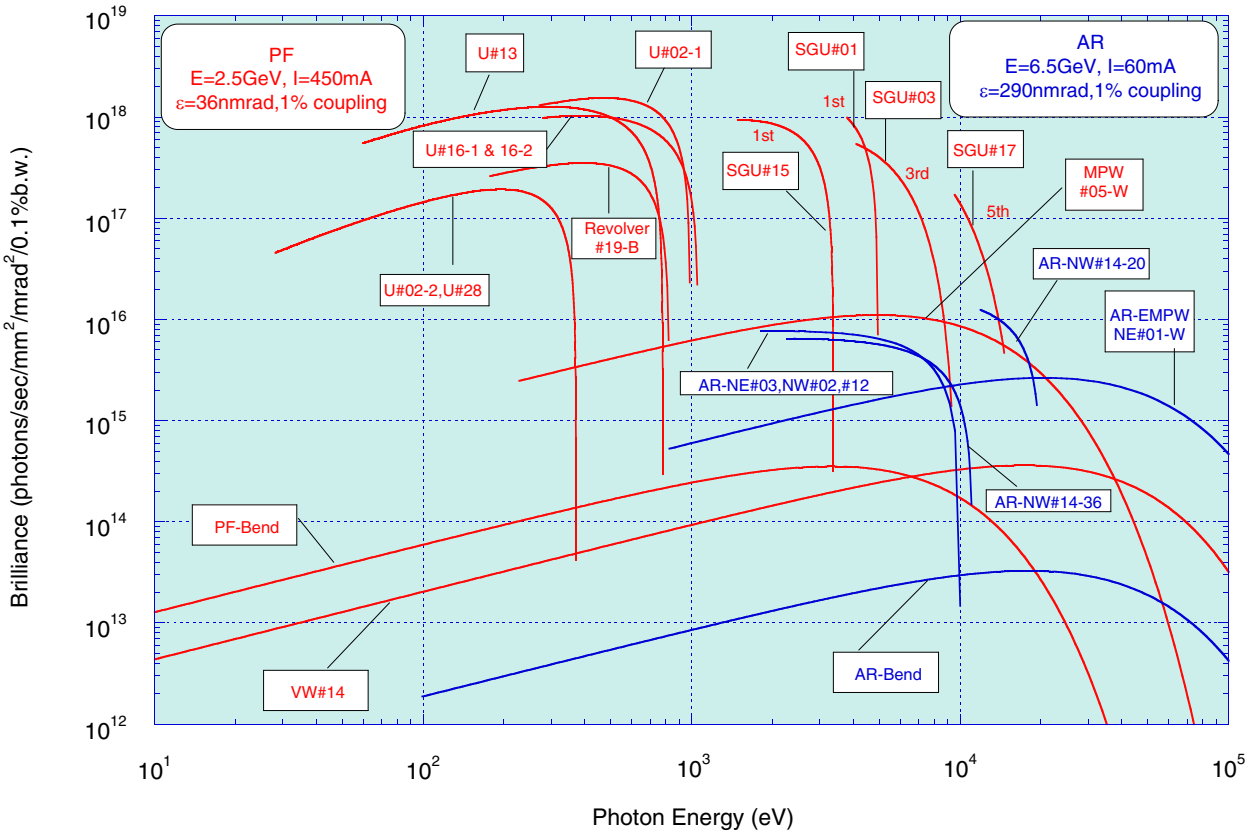

Figure 1: Synchrotron radiation spectra available at the PF Storage Ring (2.5 GeV) and the PF-AR (6.5 GeV). Brilliance of the radiation vs. photon energy are denoted by red curves for the insertion devices, SGU#01, U#02-1 & 02-2, SGU#03, MPW#05, U#13, VW#14, SGU#15, U#16-1 & 16-2, SGU#17, Revolver#19-B and U#28, and bending magnets (PF-Bend) at the PF Storage Ring. Blue curves denote those for the insertion devices, EMPW#NE01, U#NE03, U#NW02, U#NW12, U#NW14-36 and U#NW14-20, and the bending magnets (AR-Bend) at the PF-AR. The name of each source is assigned in Table 2. The spectral curve of each undulator (or undulator mode of multipole wiggler) is a locus of the peak of the first harmonic within the allowance range of K parameter. For SGU#01 and SGU#15, the fi rst harmonic regions are shown. For SGU#03, the third harmonic region is shown. For SGU#17, the fifth harmonic region is shown. Spectra of Revolver#19 for surface B are shown.

1-2 Experimental Stations

Fifty-two experimental stations are operated at the PF storage ring, the PF-AR and the slow positron facility (SPF), as shown in Figs. 2, 3, and 4. Thirty-five stations are dedicated to research using hard X-rays, 14 stations for studies in the VUV and soft X-ray energy regions, and 3 stations for studies using slow positrons. Tables 3, 4, and 5 summarize the areas of research carried out at the experimental stations at the PF storage ring, PF-AR and SPF. The specifications in terms of the optics and performance of each experimental station differ according to experimental requirements and methodology. Tables 6, 7, and 8 list the details of the optics of the hard X-ray stations, the soft X-ray/VUV stations and the slow positron stations. The principal performance parameters, including energy range, energy resolution, beam-spot size, and photon flux at the sample position for the PF and PF-AR, and energy range, pulse width, frequency, and positron flux for the SPF are shown.

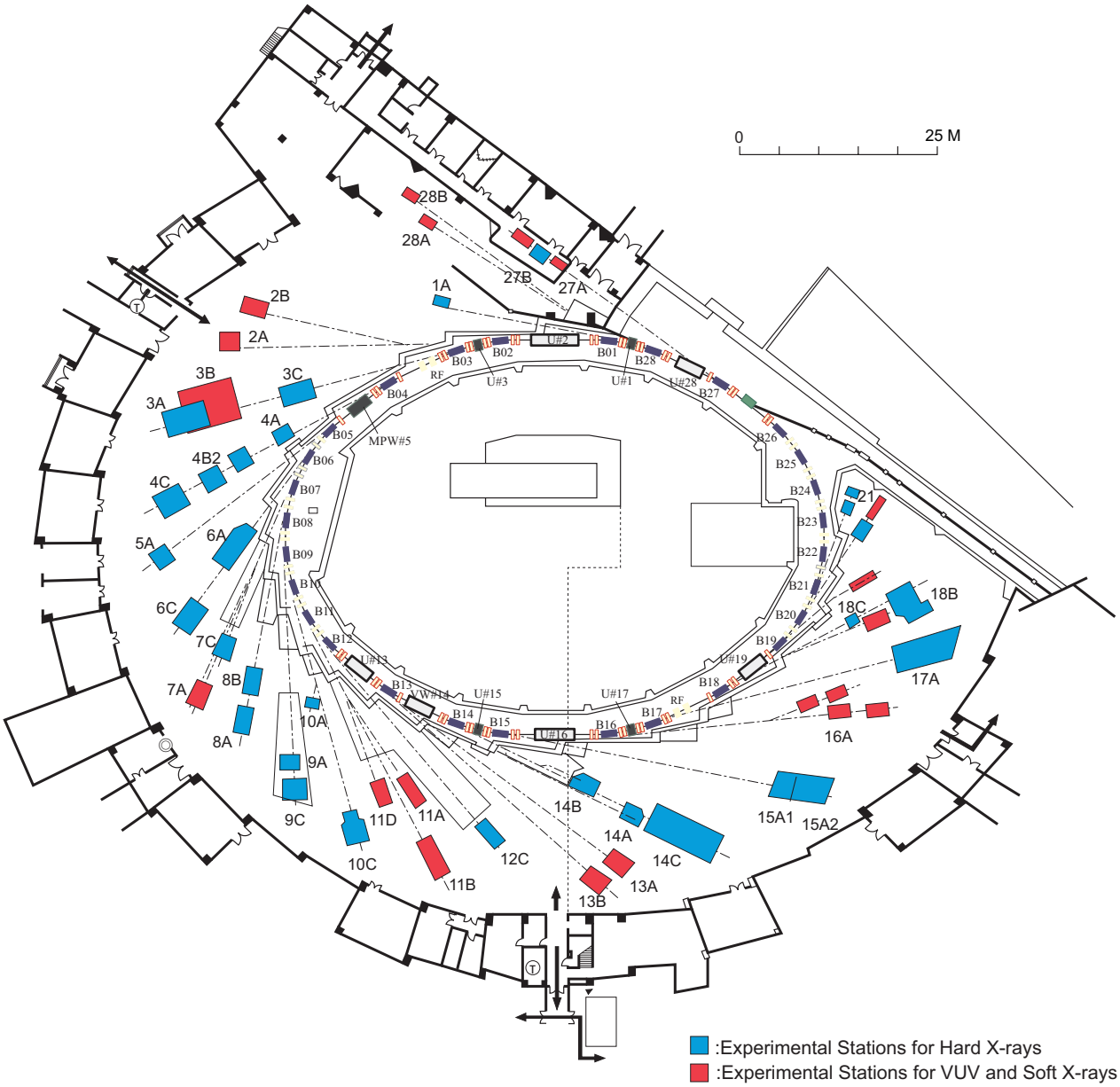

Figure 2: Plan view of the PF experimental hall, showing hard X-ray experimental stations (blue), and VUV and soft X-ray experimental stations (red).

Table 3: List of experimental stations available for users at the PF storage ring.

Experimental Station		Person in Charge
BL-1	(Short Gap Undulator)	
A	Macromolecular crystallography	N. Matsugaki
BL-2	(Undulator)	
A*	Soft X-ray spectroscopy	K. Amemiya
B*	Soft X-ray spectroscopy	K. Amemiya
BL-3	(A: Short Gap Undulator)	
A	X-ray diffraction and scattering station for materials science	H. Nakao
B	VUV and soft X-ray spectroscopy(◊)	H. Kato [Hirosaki Univ.], A. Yagishita
C	Characterization of X-ray optical elements/White X-ray magnetic diffraction	K. Hirano
BL-4		
A	Trace element analysis, X-ray microprobe	Y. Takahashi [The Univ. Tokyo], M. Kimura, Y. Niwa
B2	High resolution powder diffraction (♠)	T. Ida [Nagoya Inst. Tech.], H. Nakao
C	X-ray diffraction and scattering	H. Nakao
BL-5	(Multipole Wiggler)	
A	Macromolecular crystallography	N. Matsugaki
BL-6		
A	Small-angle X-ray scattering	N. Igarashi
C	Macromolecular crystallography	S. Sasaki [Tokyo Inst. Tech.], H. Kawata
BL-7		
A	Soft X-ray spectroscopy(♦)	J. Okabayashi [RCS], K. Amemiya
C	X-ray spectroscopy and diffraction	H. Sugiyama
BL-8		
A	Weissenberg camera for powder/Single-crystal measurements under extreme conditions	H. Sagayama
B	Weissenberg camera for powder/Single-crystal measurements under extreme conditions	H. Sagayama
BL-9		
A	XAFS	H. Abe
C	XAFS	H. Abe
BL-10		
A	X-ray diffraction and scattering(♠)	A. Yoshiasa [Kumamoto Univ.], R. Kumai
C	Small-angle X-ray Scattering	N. Shimizu
BL-11		
A	Soft X-ray spectroscopy	Y. Kitajima
B	Soft X-ray spectroscopy	Y. Kitajima
D	Characterization of optical elements used in the VSX region♠	K. Mase
BL-12		
C	XAFS	H. Nitani

Experimental Station		Person in Charge
BL-13	(Undulator)	
A/B	VUV and soft X-ray spectroscopies	K. Mase
BL-14	(Vertical Wiggler)	
A	Crystal structure analysis and detector development	S. Kishimoto
B	High-precision X-ray optics	K. Hirano
C	Medical applications and general purpose (X-ray)	K. Hyodo
BL-15	(Short Gap Undulator)	
A1	Semi-microbeam XAFS	H. Nitani
A2	High brilliance small-angle X-ray scattering	N. Shimizu
BL-16	(Variable Polarization Undulator)	
A	Soft X-ray spectroscopies with circular and linear polarization	K. Amemiya
BL-17	(Short Gap Undulator)	
A	Macromolecular crystallography	Y. Yamada
BL-18		
B	Multipurpose monochromatic hard X-ray station(♦)	A. Bhattacharyya [India,Saha Institute],R. Kumai
C	High pressure X-ray powder diffraction (DAC)(♠)	S. Nakano [NIMS], T. Kikegawa
BL-20		
A	VUV spectroscopy(◊)	N. Kouchi [Tokyo Inst. Tech], J. Adachi
B	White & monochromatic X-ray topography and X-ray diffraction experiment	H. Sugiyama
BL-27		
A	(Beamline for radioactive samples) Radiation biology, soft X-ray photoelectron spectroscopy	N. Usami
B	Radiation biology, XAFS	N. Usami
BL-28	(Elliptical / Helical Undulator)	
A	High-resolution VUV-SX beamline for angle-resolved photoemission	K. Ono
B	High-resolution VUV-SX spectroscopy	K. Ono

♠	User group operated beamline
♦	External beamline
◊	Operated by University
*	Under reconstruction
RCS:	Research Center for Spectrochemistry, the University of Tokyo
NIMS:	National Institute for Materials Science

Table 4: List of experimental stations at the PF-AR.

Experimental Station		Person in Charge
AR-NE1 A	(Multipole Wiggler) Laser-heating high pressure X-ray diffraction and nuclear resonant scattering (DAC)	T. Kikegawa
AR-NE3 A	(Undulator) Macromolecular crystallography	Y. Yamada
AR-NE5 C	High pressure and high temperature X-ray diffraction (MAX-80)	T. Kikegawa
AR-NE7 A	High pressure and high temperature X-ray diffraction (MAX-III), X-ray imaging	K. Hyodo
AR-NW2 A	(Undulator) Time-resolved Dispersive XAFS/XAFS/X-ray Diffraction	Y. Niwa
AR-NW10 A	XAFS	H. Nitani
AR-NW12 A	(Undulator) Macromolecular crystallography	Y. Yamada
AR-NW14 A	(Undulator) Time-resolved X-ray diffraction, scattering and absorption	S. Nozawa

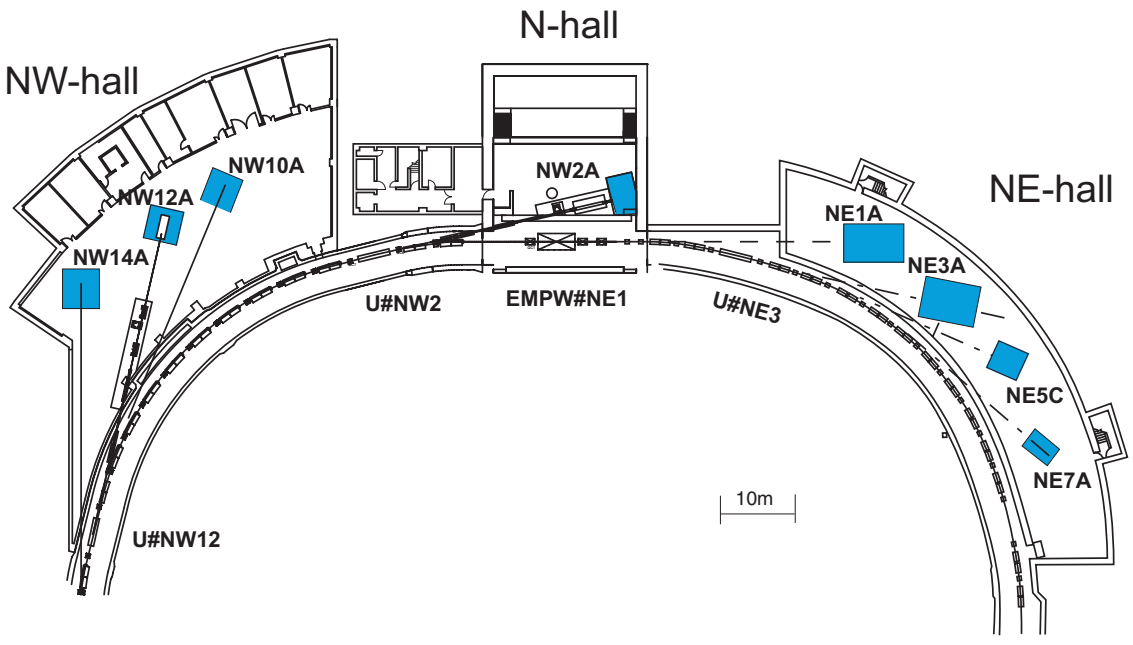

Figure 3: Plan view of beamlines in the PF-AR north-east, north, and north-west experimental halls.

Table 5: List of experimental stations at the Slow Positron Facility.

Experimental Station		Person in Charge
SPF-A3*	Total-reflection high-energy positron diffraction	T. Hyodo
SPF-B1	General purpose (Positronium negative ion)	T. Hyodo
SPF-B1	Positronium time-of-flight	T. Hyodo

* Under reconstruction

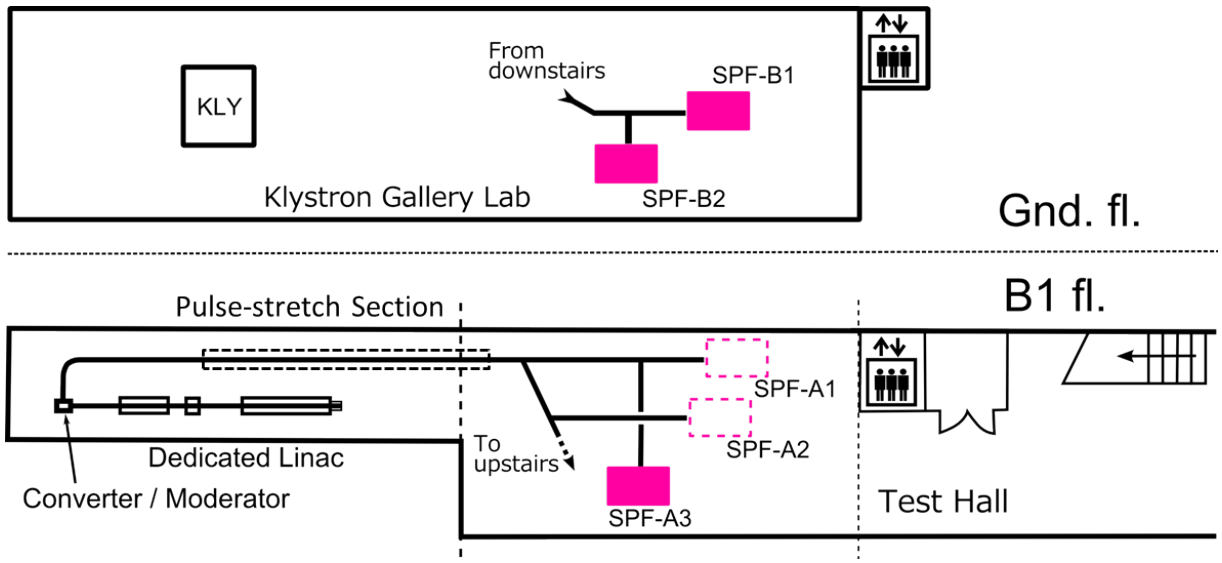

Figure 4: View of beamlines in the Slow Positron Facility.

Table 6: Specifications of X-ray beamline optics.

Branch Beamline	Horizontal Acceptance (mrad)	Type of Monochromator	Mirror	Photon Energy (keV)	Beam Size (H×V) (mm)	Photon Flux at Sample Position (/s)	Energy Resolution ($\Delta E/E$)×10^{-4}	Reference
BL-1A	0.15	Channel-Cut Si(111) Liquid N_2 Cooling	Bimorph Si Rh-Coated Si Rh-Coated	3.7 ~ 4.5 11.2 ~ 12.9	0.05×0.01	4×10^{11}@11.2 keV (0.025×0.01mm^2)	~2	
BL-3A	1	Flat Double Crystal Si(111)	Bent Cylinder	4 ~ 14	0.7×0.2	6×10^{12}	~5	1, 2
BL-3C	1.75	Double Crystal Si(111)	None	4 ~ 20 or white	20×6(mono) 0.1x0.1(white)		~2	
BL-4A	6	Double Crystal Si(111)	KB mirror polycapillary	4 ~ 20	0.005×0.005 0.03×0.03		~2	3
BL-4B2	4.5	Flat Double Crystal Si(111)	Bent Cylinder	6 ~ 20	13×2		~2	4, 5
BL-4C	2	Flat Double Crystal Si(111)	Bent Cylinder	5 ~ 19	0.7×0.5		~5	6, 7
BL-5A	0.5	Micro-Channel Double Crystal Si(111)	Bent Plane Si Rh-Coated Bent Cylinder Si Rh-Coated	6.5 ~ 17	1.2×0.4	3×10^{11} (0.2×0.2mm^2)	~2	
BL-6A	2	Bent Crystal Ge(111) (α = 8.0°)	Bent Cylinder ULE	8.3 (fixed)	0.5×0.2	1.0×10^{12}/mm^2 (Slit full-open)	~10	8
BL-6C	2	Flat Double Crystal Si(111)	Bent Cylinder	5 ~ 20 (~25 non-Focus)	0.5×0.3			
BL-7C	4	Double Crystal Si(111) Sagittal Focusing	Double Mirror Fused Quartz Focusing	4 ~ 20 (4 ~ 13)	5×1	1×10^{10}/6mm^2 (8keV, 300mA) (1×10^{11} when focused)	~2	9 - 11
BL-8A	2.22	Flat Double Crystal Si(111)	Bent Cylinder	5 ~ 19	0.82×0.52	3.2×10^{11} (12.4keV, 400mA)	~5	12
BL-8B	2.21	Flat Double Crystal Si(111)	Bent Cylinder	5 ~ 19	0.75×0.45	2.2×10^{11} (12.4keV, 400mA)	~5	12
BL-9A	3	Double Crystal Si(111)	Collimating and Focusing Bent Conical Mirrors Rh-Coated Double Flat Mirror Ni-Coated		0.5×0.3	6×10^{11}(7keV, 450mA)	2	13,14
BL-9C	3.5	Double Crystal Si(111)	Bent Cylinder Rh-Coated Si	4 ~ 23		1×10^{11}(8keV, 450mA)	~2	

Branch Beamline	Horizontal Acceptance (mrad)	Type of Monochromator	Mirror	Photon Energy (keV)	Beam Size (H×V) (mm)	Photon Flux at Sample Position (/s)	Energy Resolution ($\Delta E/E$)×10^{-4}	Reference
BL-10A	1	Si(111),Si(311) Quartz(100) PG(002) Curved Si(111) (α~ 4°, 8°)	Plane Pt Coated Fused Quartz	5 ~ 25	10×3		10 -5	15
BL-10C	2.1	Fix-Exit Double Crystal Si(111)	Bent Cylinder Rh-Coated	6 ~ 14	0.63×0.18	1.5 x 10^{11} (8 keV)	2	
BL-12C	2	Double Crystal Si(111)	Bent Cylinder Double Flat Mirror Ni-Coated	4 ~ 23	0.6×0.6	9 x 10^{10} (8 keV,450mA)	-2	16
BL-14A	1.28 (Vertical)	Double Crystal Si(111) Si(311) Si(553)	Bent Cylinder Rh-Coated Fused Quartz	5.1 ~ 19.1 9.9 ~ 35.6 22.7 ~ 84.5	2×1 at focus 5×38		2	17
BL-14B	2.2 (Vertical)	Flat Double Crystal Si(111)	None	10 ~ 57	5×14		2	18
BL-14C	1.96 (Vertical)	Double Crystal Si(111),Si(220)	None	5 ~ 100 or white	6×70		2	19,20
BL-15A1	0.2	Double Crystal Si(111) Liquid N_2 Cooling	Horizontal: Bent Plane Si Bimorph Silica Rh-Coated Vertical: Bent Plane Si Rh-Coated Double Flat Si Ni-Coated	2.1 ~ 15	0.02×0.02	3.5 x 10^{11}	-2	21
BL-15A2					0.6×0.04	(7.5 keV, 450mA)		
BL-17A	0.1 ~ 0.2	Double Crystal Si(111) Liquid N_2 Cooling	Bent Plane Si Rh-Coated Bent Plane Si Rh-Coated	6 ~ 13	0.25×0.04	10^{10} (12.4 keV,450mA, 0.02×0.02mm^2)	-2	22 - 24
BL-18B [India, DST]	2	Double Crystal Si(111)	Plane and Bent Cylinder	6 ~ 20			-2	
BL-18C	1	Double Crystal Si(111)	Cylinder Fused Quartz Pt-Coated	6 ~ 25	0.07×0.04		-2	
BL-20B	2	Double Crystal Si(111)	None	5 ~ 25 or white	26×5	1x 10^{11} (12 keV,450mA)	-2	
BL-27B	4	Double Crystal Si(111)	None	4 ~ 20	100×6		-2	25

Branch Beamline	Horizontal Acceptance (mrad)	Type of Monochromator	Mirror	Photon Energy (keV)	Beam Size (H×V) (mm)	Photon Flux at Sample Position (/s)	Energy Resolution ($\Delta E/E \times 10^{-4}$)	Reference
AR-NE1A	0.28	Micro-Channel Double Crystal Si(111), High-Resolution Channel Cut Si(4,2,2)&(12,2,2)	Bent Plane W/C Multilayer Coated Si	6~ 50	0.8×0.2	8×10^{11} ($0.2\times0.2mm^2$)	-2	
AR-NE3A	H:0.2 V:0.1	Double Crystal Si(111) Liquid N_2 Cooling	Pre-Mirror Bent Flat Si Rh-Coated Post-Mirror Bent Cylinder Fused Quartz Rh-Coated	6.5 ~ 17	0.8×0.2	8×10^{11} ($0.2\times0.2mm^2$)	-2	26, 27
AR-NE5C	3	Double Crystal Si(111)	None	30 ~ 100 or white	60×5		5	28
AR-NE7A	4			25 ~ 50 or white	80×3		5	
AR-NW2A	H:1.0 V:0.2	Double Crystal Si(111) Liquid N_2 Cooling	Bent Cylinder Si Rh-Coated Bent Flat Si Rh-Coated	5 ~ 25 or white	0.6×0.2 ~10×0.06	6×10^{12} (12keV, 60mA)	-2	29 - 31
AR-NW10A	1.2	Si(311)	Pt-Coated Bent Cylinder Double Flat Mirror Rh-Coated	8 ~ 42	2.2×0.5	1×10^{10} (12keV, 60mA)	-1	32
AR-NW12A	H:0.3 V:0.1	Double Crystal Si(111) Liquid N_2 Cooling	Pre-Mirror Bent Flat Si Rh-Coated Post-Mirror Bent Cylinder Si Rh-Coated	6.5 ~ 17	1.3×0.3	2×10^{11} ($0.2\times0.2mm^2$)	-2	33 - 35
AR-NW14A	H:0.3 V:0.1	Double Crystal Si(111) Liquid N_2 Cooling	Bent Cylinder Rh-Coated Bent Flat Rh-Coated	4.9 ~ 25	0.45×0.25	1×10^{12}	-2	36

India DST: Department of Science & Technology

REFERENCES

[1] *Photon Factory Activity Report 2006*, **#24**, A 64 (2008).
[2] *Photon Factory Activity Report 2006*, **#24**, A 104 (2008).
[3] A. Iida et *al., Rev. Sci. Instrum.* **66**, 1373 (1995).
[4] Powder Diffraction User Group, KEK Report **94-11** (1995).
[5] H. Toraya, H. Hibino, and K. Ohsumi, *J. Synchrotron Rad.* **3**, 75 (1996).
[6] H. Iwasaki *et al., Rev. Sci. Instrum.* **60**, 2406 (1989).
[7] *Photon Factory Activity Report 1995* **#13**, E-1 (1996).
[8] N. Shimizu *et al., J. Phys.: Conf. Ser.* **425**, 202008 (2013).
[9] M. Nomura and A.Koyama, *KEK Internal*, **93-1** (1993).
[10] M. Nomura *et al., KEK Report*, **91-1** (1991).
[11] M.Nomura and A.Koyama, in *"X-ray Absorption Fine Structure"*, ed. by S. S. Hasnain, Ellis Horwood, Chichester, **667** (1991).
[12] A. Nakao *et al., AIP Conf. Proc.* **1234**, 367 (2010).
[13] M. Nomura and A. Koyama, *J. Synchrotron Rad.* **6**, 182 (1999).
[14] M. Nomura and A. Koyama, *Nucl. Instrum. Meth.* **A467-468**, 733(2001).
[15] S. Sasaki, *Rev. Sci. Instrum.* **60**, 2417 (1989).
[16] M. Nomura and A. Koyama, *KEK Report,* **95-15** (1996).
[17] Y. Satow and Y. Iitaka, *Rev. Sci. Instrum.* **60**, 2390 (1989).
[18] M. Ando *et al., Nucl. Instrum. Meth.* **A246**, 144 (1986).
[19] *Photon Factory Activity Report 1999*, **#17**, A 92 (2000).
[20] *Photon Factory Activity Report 1999*, **#17**, A 103 (2000).
[21] N. Igarashi *et al., J. Phys.: Conf. Ser.* **425**, 072016 (2013).
[22] N. Igarashi *et al., AIP Conf. Proc.* **879**, 812 (2007).
[23] N. Igarashi *et al., J. Synchrotron Rad.* **15**, 292 (2008).
[24] Y. Yamada *et al., J. Synchrotron Rad.* **20**, 938 (2013).
[25] H. Konishi *et al., Nucl. Instrum. Meth.* **A372**, 322 (1996).
[26] Y. Yamada *et al., AIP Conf. Proc.* **1234**, 415 (2010).
[27] M. Hiraki *et al., AIP Conf. Proc.* **1234**, 673 (2010).
[28] T. Kikegawa *et al., Rev. Sci. Instrum.* **66**, 1335 (1995).
[29] T. Mori *et al., AIP Conf. Proc.* **705**, 255 (2004).
[30] H. Kawata *et al., AIP Conf. Proc.* **705**, 663 (2004).
[31] Y. Inada *et al., AIP Conf. Proc.* **879**, 1230 (2007).
[32] M. Nomura *et al., AIP Conf. Proc.* **882**, 896 (2007).
[33] L. M. G. Chavas *et al., J. Synchrotron Rad.* **19**, 450 (2012).
[34] L. M. G. Chavas *et al., J. Phys.: Conf. Ser.* **425**, 012008 (2013).
[35] L. M. G. Chavas *et al., J. Synchrotron Rad.* **20**, 838 (2013).
[36] S. Nozawa *et al., J. Synchrotron Rad.* **14**, 313 (2007).

Table 7: Specifications of VUV and soft X-ray beamline optics.

Branch Beamline	Acceptance H × V (mrad) or Undulator Parameters	Type of Monochromator	Groove Density (/mm)	Energy Range (eV)	Beam Size H × V (mm)	Resolving Power (E/ΔE) Photon Flux (photons/s)	Reference
BL-2A* Undulator	ID02: K_{max} = 2.3, λ_u = 6 cm ID022: K_{max} = 5.0, λ_u = 16 cm	Variable-Included-Angle Varied-Line-Spacing Plane Grating	400 600 1000	30 ~ 2000	~0.5 × 0.1	2000 ~ 20000 10^{13} ~ 10^{11}	1
BL-2B* Undulator	ID02: K_{max} = 2.3, λ_u = 6 cm ID022: K_{max} = 5.0, λ_u = 16 cm	Variable-Included-Angle Varied-Line-Spacing Plane Grating Double Crystal InSb(111), Ge(111), Si(111)	400 600 1000	30 ~ 4000	~0.5 × 0.1	2000 ~ 20000 10^{13} ~ 10^{11}	1
BL-3B	10 × 2	Grazing Incidence R = 24 m α+β = 165° 1800	200 600	10 ~ 280	< 2ϕ	200 ~ 3000 10^{12} ~ 10^{9}	2, 3
BL-7A [RCS]	6 × 1	Varied-Line-Space Plane Grating	150 300 650	50 ~ 1300	2.5 × 0.5	1000 ~ 9000 10^{12} ~ 10^{9}	4
BL-11A	5 × 1	Varied-Included-Angle Varied-Line-Spacing Plane Grating	600 1200	70 ~ 1900	2 × 1	500 ~ 5000 10^{12} ~ 10^{9}	
BL-11B	4 × 0.6	Double Crystal InSb (111), Si (111)		1724 ~ 5000	5 × 2	2000 10^{10}	5 - 7
BL-11D	4 × 2	Grazing Incidence Varied Deviation-Angle On-Blaze Mount R_1 = 52.5 m R_3 = 22.5 m	2400	60 ~ 245 200 ~ 900	1 × 0.1	2000 10^{11}	8, 9
BL-13A/B Undulator	K_{max} = 8 λ_u = 18 cm	Variable-Included-Angle Varied-Line-Spacing Plane Grating	300 1000	30 ~ 330 100 ~ 1600	~0.2 × 0.04	4000 ~ 10000 10^{12} ~ 10^{9}	10 - 12
BL-16A Undulator	K_{max} = 2.37 (Circular Polarization) K_{max} = 3.12 (Horizontal Linear Polarization) K_{max} = 1.98 (Vertical Linear Polarization) K_{max} = 1.73 (45-deg Linear Polarization) λ_u = 5.6 cm	Variable-Included-Angle Varied-Line-Spacing Plane Grating	500 1000	250 ~ 1500	~0.2 × 0.1	4000 ~ 8000 10^{12} ~ 10^{11}	13, 14
BL-19B Revolver Undulator	K = 0.5 ~ 1.25 λ_u = 5 cm	Varied-Line-Space Plane Grating	800 2400	200 ~ 1200	1 × 0.5	4000 ~ 8000 10^{12} ~ 10^{11}	15 - 17
BL-20A	28 × 5	3m Normal Incidence	1200 2400	5 ~ 40	2 × 1	300 ~ 30000 10^{12} ~ 10^{8}	18
BL-27A	5 × 0.5	Double Crystal InSb (111)		1800 ~ 4000		2000	19
BL-28A/B Helical Undulator	K_x = 0.23 ~ 3 K_y = 0.23 ~ 6 K_y = 0.23 ~ 6	Varied-Line-Space Plane Grating	400	30 ~ 300	0.15 × 0.05	30000 10^{12}	1

* Under reconstruction

RCS: Research Center for Spectrochemistry, the University of Tokyo

REFERENCES

[1] K. Amemiya and T. Ohta, *J. Synchrotron Rad.* **11**, 171 (2004).
[2] A. Yagishita *et al., Nucl. Instrum. Meth.* **A306**, 578 (1991).
[3] S. Masui *et al., Rev. Sci. Instrum.* **63**, 1330 (1992).
[4] K. Amemiya *et al., J. Elec. Spectrosc. Relat. Phenom.* **124**, 151 (2002).
[5] T. Ohta *et al., Nucl. Instrum. Meth.* **A246**, 373 (1986).
[6] M. Funabashi *et al., Rev. Sci. Instrum.* **60**, 1983 (1989).
[7] T. Iwazumi *et al., Rev. Sci. Instrum.* **66**, 1691 (1995).
[8] *Photon Factory Activity Report 1997* **#15**, A 101 (1998).
[9] T. Hatano and S. Aihara, *J. Phys.: Conf. Ser.* **425**, 152018 (2013).
[10] K. Mase *et al., AIP Conf. Proc.* **1234**, 709 (2010).
[11] A. Toyoshima *et al., J. Vac. Soc. Jpn.* **54**, 580 (2011).
[12] A. Toyoshima *et al., J. Phys.: Conf. Ser.* **425**, 152019 (2013).
[13] K. Amemiya *et al., AIP Conf. Proc.* **1234**, 295 (2010).
[14] K. Amemiya *et al., J. Phys.: Conf. Ser.* **425**, 152015 (2013).
[15] S. Suzuki *et al., Activity Report of SRL-ISSP* **60**, (1989).
[16] A. Kakizaki *et al., Rev. Sci. Instrum.* **60**, 1893 (1989).
[17] A. Kakizaki *et al., Rev. Sci. Instrum.* **63**, 367 (1992).
[18] K. Ito *et al., Rev. Sci. Instrum.* **66**, 2119 (1995).
[19] H. Konishi *et al., Nucl. Instrum. Meth.* **A372**, 322 (1996).

Table 8: Specifications of the beamlines at Slow Positron Facility.

Beamline	Beam Energy	Pulse Width	Frequency	Intensity	Reference
SPF-A3*	100eV - 35keV	1μs	≤ 50Hz	$5x10^7$ e+/s ($5x10^6$ e+/s after brightness enhancement)	3,4
SPF-B1	100eV - 35keV	1-10ns	≤ 50Hz	$5x10^6$ e+/s	1,2,3,4
SPF-B2	100eV - 35keV	1-10ns	≤ 50Hz	$5x10^6$ e+/s	5,6

* Under reconstruction

REFERENCES

[1] T. Tachibana, *et. al., Nucl. Instrum. Methods Phys. Res., Sect.* **A 621**, 670 (2010).
[2] K. Michishio, *et al., Phys. Rev. Lett.* **106**, 153401 (2011).
[3] K. Wada, *et al., Eur. Phys. J. D* **66**, 37 (2012).
[4] K. Michishio, *et al., Appl. Phys. Lett.* **100**, 254102 (2012).
[5] K. Wada, *et al., J. Phys.: Conf. Ser.* **443**, 012082 (2013).
[6] H. Terabe, S. Iida, K. Wada, T. Hyodo, A. Yagishita, and Y. Nagashima, *J. Phys.: Conf. Ser.* **443**, 012075 (2013).